

Investigating internal structure of permafrost using conventional methods and ground-penetrating radar at Honhor basin, Mongolia

Tonghua Wu · Qinxue Wang · Lin Zhao ·
Erji Du · Wu Wang · Ochirbat Batkhisig ·
Dorjgotov Battogtokh · Masataka Watanabe

Received: 18 May 2011 / Accepted: 1 March 2012
© Springer-Verlag 2012

Abstract A ground-penetrating radar (GPR) survey was conducted at the end of August 2009 in the suburb region of Ulaanbaatar, Honhor basin, Mongolia, in combination with conventional methods such as borehole drilling and measurement of ground temperatures. The interface of frozen and unfrozen sediment was distinctly resolved in the interpreted GPR images, verified by the borehole drilling records and 6-month measurement of ground temperatures. The location of the permafrost table was assessed to be at the depth of 2–4 m in the study region. A conspicuous ice-saturated soil layer (massive ground ice) was detected in the interpreted GPR images with a thickness of 2–5 m. The GPR investigation results were consistent with the borehole drilling records and ground temperatures observation. The borehole logs and ground temperatures profile in the borehole indicates that permafrost at Honhor basin is characterized by high ground temperature and high ice content, which implies that ongoing climatic warming would have great

influence on permafrost dynamics. The research results are of great importance to further assess permafrost dynamics to climatic change in the boundary of discontinuous and sporadic permafrost regions in Mongolia in the future.

Keywords Permafrost · Borehole drilling · Ground-penetrating radar · Honhor basin · Mongolia

Introduction

Permafrost (soil or rock whose temperature remains at or below 0 °C for 2 y or more) is a typical landform in Mongolia. Mongolia is in the southern fringe of the continuous Siberian permafrost zone, and approximately two-thirds of its territory was characterized by permafrost regions (Tumurbaatar and Mijiddorj 2006). Previous studies indicated that the mean annual air temperature in Mongolia has increased by 1.66 °C from 1960 to 2001 (Batima et al. 2005), which exceeds double of the global average increase (0.7 °C) in the last century reported by IPCC (2007). The pronounced permafrost degradation has been observed during recent years in the long-term measurement of the thermal regime of permafrost in Mongolia, especially in the discontinuous permafrost regions (Sharkhuu 2003; Sharkhuu et al. 2008; Ishikawa et al. 2005; Zhao et al. 2010).

Ground-penetrating radar (GPR) has been applied extensively in periglacial investigation during the past decades and turned out to be an effective, non-invasive geophysical tool in permafrost environments (Arcone et al. 1998, 2002; Hinkel et al. 2001; Moorman et al. 2003; Wu et al. 2005, 2009; Doolittle and Nelson 2009). Ground-penetrating radar works especially well in detecting the active layer thickness (Arcone et al. 1998; Hinkel et al. 2001; Wu et al. 2005), identifying the massive ground ice

T. Wu · L. Zhao · E. Du · W. Wang
Cryosphere Research Station on the Qinghai-Tibet Plateau,
State Key Laboratory of Cryospheric Sciences, Cold and Arid
Regions Environmental and Engineering Research Institute,
Chinese Academy of Sciences, Lanzhou, 730000, China

Q. Wang (✉)
Center for Regional Environmental Research, National Institute
for Environmental Studies, 16-2 Onogawa,
Tsukuba 305-8506, Japan
e-mail: wangqx@nies.go.jp

O. Batkhisig · D. Battogtokh
Institute of Geography, Mongolian Academy of Sciences,
Ulaanbaatar 210-620, Mongolia

M. Watanabe
Graduate School of Media and Governance, Keio University,
5522 Endo, Fujisawa, Kanagawa 252-8520, Japan

bodies (Yoshikawa et al. 2006; Brandt et al. 2007; De Pascale et al. 2008), and resolving the interfaces between frozen and unfrozen soil layers (Stevens et al. 2009). With the calibration of direct observations (e.g., borehole drilling, test pit excavation, and ground temperatures measurement), GPR could accurately map the internal structure and characteristics of ice content of permafrost and extend the point-sampling surveying results to obtain the spatial features of permafrost on a regional scale.

This study intends to apply conventional methods and GPR to investigate the vertical distribution and structure of permafrost in the typical discontinuous permafrost regions at Honhor basin of Mongolia. The locations of the permafrost table, massive ground ice, and permafrost thickness will be assessed and the vertical distribution of ice contents in permafrost will be revealed in this region. The investigation results will be counted on to provide fundamental knowledge for further assessment response of permafrost to climatic changes in the future.

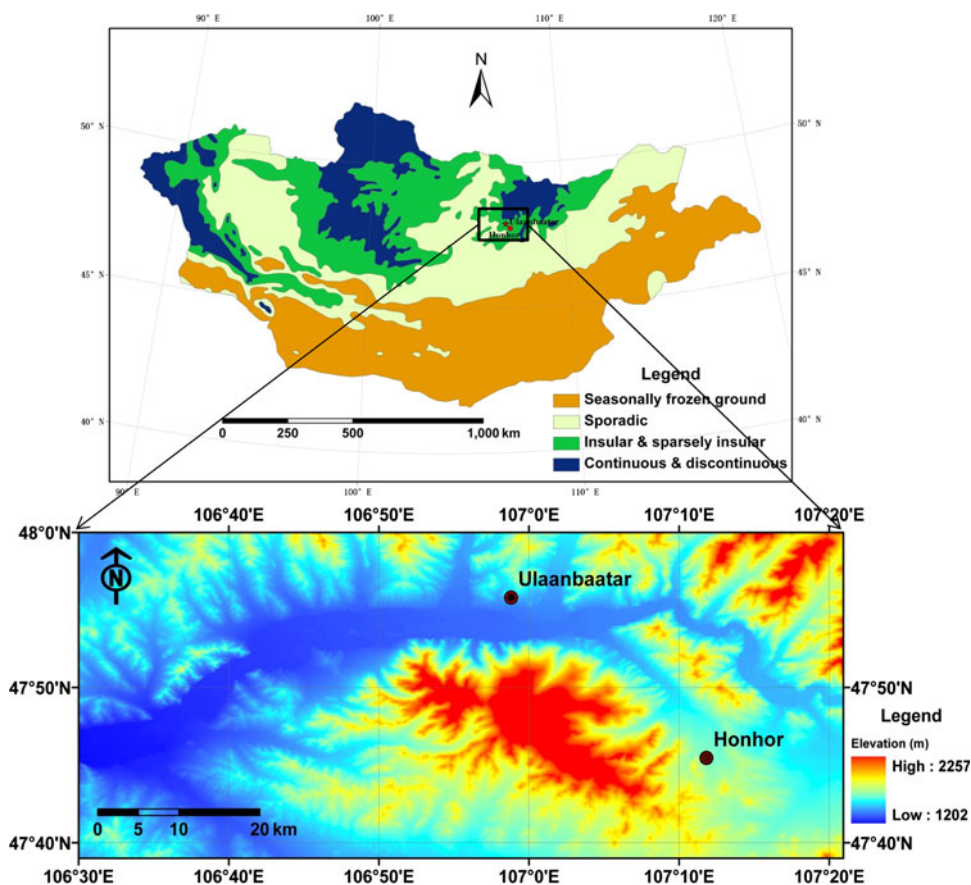
Study area and methods

Honhor is in the boundary regions between discontinuous and sporadic permafrost regions, which is about

12 km southeast of Ulaanbaatar, Mongolia ($47^{\circ}41'32.5''\text{N}$, $108^{\circ}15'34.7''\text{E}$, 1342 m above the sea level). The study site is located in a northwest-southeastward intermontane basin, south of the Khentei mountains range (Fig. 1). Previous observation indicates that the permafrost temperatures approximate to 0°C and are thermally unstable in this region (Ishikawa et al. 2005; Sharkhuu 2003). Based on the assessment of Sharkhuu (2003), permafrost in the study region is vulnerable to occurring climatic warming and the ground temperatures were increasing at a rate of $0.01^{\circ}\text{C}/\text{y}$ in the surrounding regions. In northeast China at the same latitude, the southern limit of permafrost has moved northwards on the way that sporadic permafrost disappeared, discontinuous permafrost became sporadic and some of the continuous permafrost regions became discontinuous (Jin et al. 2007).

The mean annual air temperature (MAAT) in the study region was -1.4°C , and the mean air temperature in summer and winter was 18.0 and -22.8°C , respectively. In Ulaanbaatar, an increase of MAAT of $0.052^{\circ}\text{C}/\text{y}$ ($P < 0.001$) has been observed over the period 1961–2009 (Fig. 2), which could exert pronounced impacts on the thermal regime of permafrost. The mean annual total precipitation of Ulaanbaatar meteorological station was about 235 mm, 53.3 % of which fell from June to August.

Fig. 1 A relief map showing the location of Honhor site in Mongolia (permafrost distribution map was drawn after Sodnom and Yanshin 1990)



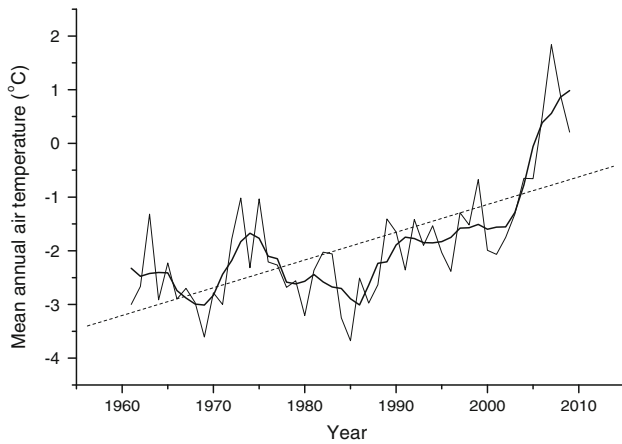


Fig. 2 Time series in MAAT for the 1961–2009 period. The *bold line* is the 5-year running average and the *dashed line* is the linear trend of mean annual air temperature

The underlying vegetation was primarily comprised of sparse grass with maximum coverage of 40–60 % in August. The soil texture of ground surface above 5 cm depth consists of dry loamy sands with little organic matter. The terrain is relatively smooth. There are small ponds in the middle of the basin, which possibly result from occurrence of a thermokarst slump. The study area has long been herded by nomadic people, while in recent years human activities are increasing due to its adjacency to the capital. Therefore, this site was selected for monitoring the long-term permafrost changes responding to climatic warming.

In this study, the geophysical investigation was conducted in tandem with the borehole drilling on 21 August of 2009, the warmest season in Mongolia. The seasonal thawing depth was presumed to approach maximum in an annually fluctuating cycle. Two GPR investigation transects were deployed from east to west through the basin. The long transect starts from the foot of the eastern hill,

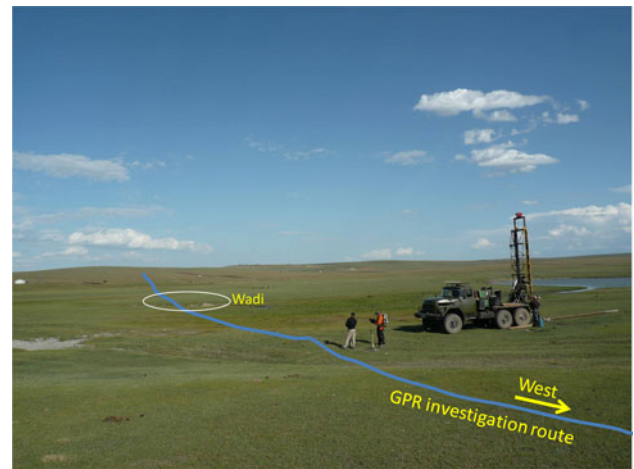


Fig. 3 The longitudinal transect from east to west across the Honhor basin

extending for about 2.4 km (Fig. 3), and ends at the foot of the western hill. This transect was designed for the purpose of acquiring general knowledge of the internal structure and distribution of permafrost in the basin. The other short transect (68 m long) is deployed to know about the detailed information about permafrost in the middle of the basin. The Mala Professional Explorer (ProEx) radar system, manufactured by Mala Geoscience of Sweden, has been used for the present study. The GPR system was equipped with 100 MHz unshielded Rough Terrain Antenna (RTA) for the 2.4 km long transect (Fig. 4a) and 100 MHz shielded antenna for the 68 m long transect (Fig. 4b). The measurements using 100 MHz center frequency unshielded antenna were triggered at a constant spacing of 1 m behind a car at a relatively steady traveling speed (about 1 m/s) (Fig. 4a). The distance between the control unit and the RTA was kept separated about 5 m away from each other to avoid interference from the metal objects of the car.



Fig. 4 The GPR investigation with 100 MHz shielded board-shaped antenna across a 68 m long transect near the borehole (a) and 100 MHz RTA across the continuous 2.4 km, east-to-west transect (b)

The 100 MHz shielded antenna GPR investigation was conducted by three persons along the transect (Fig. 4b). A sampling time window of 470 ns was used for the 100 MHz antenna, providing a maximum penetration depth of 23.5 m.

The 2-D data analysis module of REFLEXW 5.5 software (Sandmeier 2010) was used to carry out the post processing of raw GPR data. The post-processing steps of the GPR images include static correction to eliminate the time delay between trigger and recording, energy decay gain to enhance the signal-to-noise ratio, DC subtraction to remove the initial low-frequency noise, bandpass filter to remove high-frequency noise, subtracting average to remove unwanted background noise, and topographic correction to enhance the visualization for interpretation. The average propagation velocity (0.10 m/ns) for converting the travel time of electromagnetic wave to depth was estimated by direct measurements of the two-way travel time to the soil cores, which obtained in the drilling borehole in the middle of the short transect. The common midpoint (CMP) measurement was carried out along the first 50 m of transect using 100 MHz shielded antenna. The interface between frozen and thawed soil layers in the soil cores was used to estimate the average propagation velocity of the radar waves. The resolution of GPR at 100 MHz central frequency antenna with a velocity of 0.10 m/ns is estimated to be 0.25–0.50 m.

While the GPR investigation was conducted, a 10 m deep borehole was drilled in the middle of the short GPR investigation transect for long-term measurement of permafrost temperatures and to calibrate the results of the geophysical investigations as well. The drilling of a 10 m deep borehole was performed using the dry-drilling method in 4 h. The drilling head has been pulled out once penetrating downward 50 cm and corresponding description of the structure of soil cores was archived. A string of thermistors including 20 sensors was put in the borehole to measure ground temperatures on 28 August 2010. The 20 thermistor sensors were placed 0.5 m apart in depth in the string and manufactured by the State Key Laboratory of Frozen Soil Engineering, Chinese Academy of Sciences. The accuracy of measured ground temperatures is estimated to be ± 0.05 °C. The data are collected automatically by Campbell Scientific data-logger CR800 at an interval of 1 h (Fig. 5).

Results and discussion

Conventional drilling and ground temperatures observation

The borehole drilling revealed that clay is the dominant soil texture at this site, with occasional coarse-grained sand



Fig. 5 The observation system of ground temperatures, which includes a 10 m long thermistors string, a Campbell Scientific data-logger, and a laptop

in the soil core. The stratigraphy and soil texture for each layer is shown in Fig. 6. Six layers were identified according to the internal composition, texture, and ice content of sampled soil cores. The drilling showed that the icy soil layer is located at the depth of about 4.0 m below a layer of humid and cemented clay, with moderate ice content in the sandy and gravelly soil. Underlying a 20–30 cm thick sandy and gravelly frozen soil layer, an ice-rich clay layer exists for a thickness of about 4.7 m (between the depth of 4.3 and 9.0 m), and the ice volume pronouncedly increases with the downward depth (Fig. 7). Between the depths of 9.0–10.0 m, the ice content of the soil cores approaches to be saturated, displaying in the formation of massive ground ice (Fig. 7).

Figure 8 shows the monthly ground temperature profiles which were measured from September 2010 to February 2011. The maximum thawing depth has reached a depth of 3.0 m. Compared with the logged results of soil cores, permafrost at the depth of 3.0–4.0 m could be expected to contain unfrozen water because the ground temperature at the depth of 3.5 m was close to 0 °C. The location of permafrost table is estimated to be at the depth of about 3.5 m. The lowest ground temperature was observed on 3 September 2010 at the depth of 5.5 m, which amounts to -1.2 °C. As for the monthly ground temperatures in the borehole, the lowest ground temperature (-1.0 °C) was observed in October at the depth of 6.0 m. Based on the inference of monthly ground temperature gradient (0.05 °C/m) beneath the depth of 6 m in October, the depth of permafrost base is estimated to be 24 m, which indicated that the thickness of permafrost layer amounts to about 20 m at this site. The observed ground temperatures at all levels are higher than -1.0 °C, which indicated a thermal regime of permafrost is vulnerable to ongoing climatic changes in this region. In the

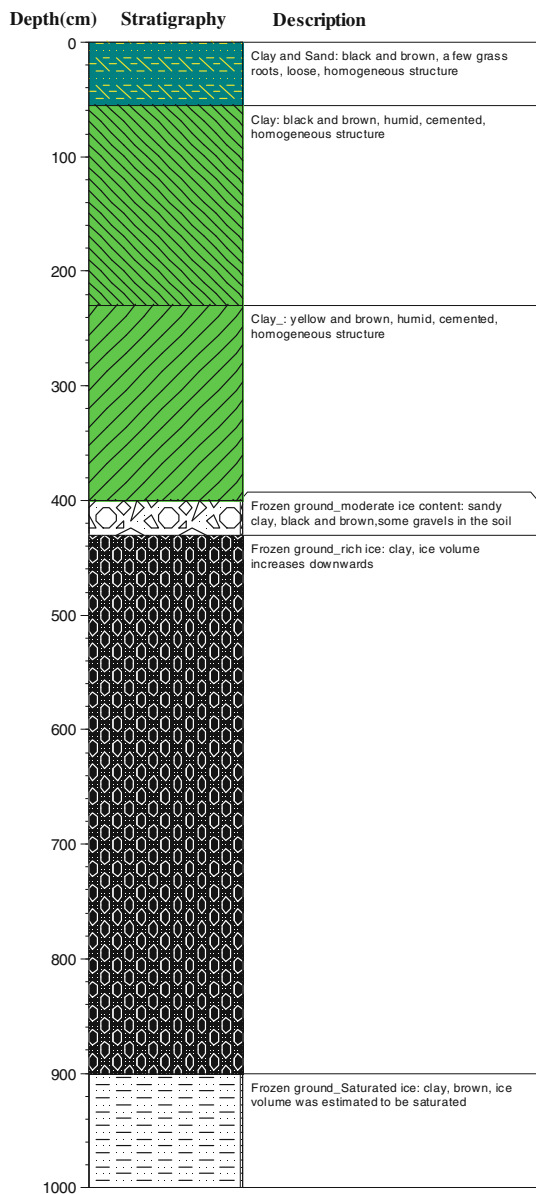


Fig. 6 In situ logged borehole profile shows the lithological texture and ice content of soil cores

Fig. 7 The sampled soil cores at the in situ drilled borehole, which indicate an increase of ice content with the depth



context of climatic warming occurring in Mongolia, there is an increasing concern about the permafrost degradation in the steppe regions, which could induce grassland deterioration and desertification (Yang et al. 2004).

Ground-penetrating radar (GPR)

Figure 9a shows the interpreted GPR image of the 64 m long transect about 5 m west away from the in situ drilling

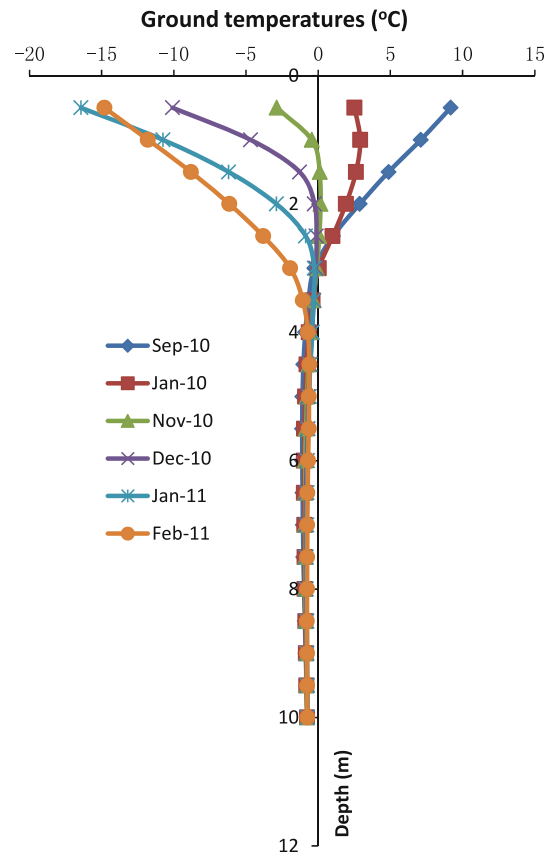


Fig. 8 Ground temperature profile observed from the deployed thermistors string at an interval of 0.5 m in depth

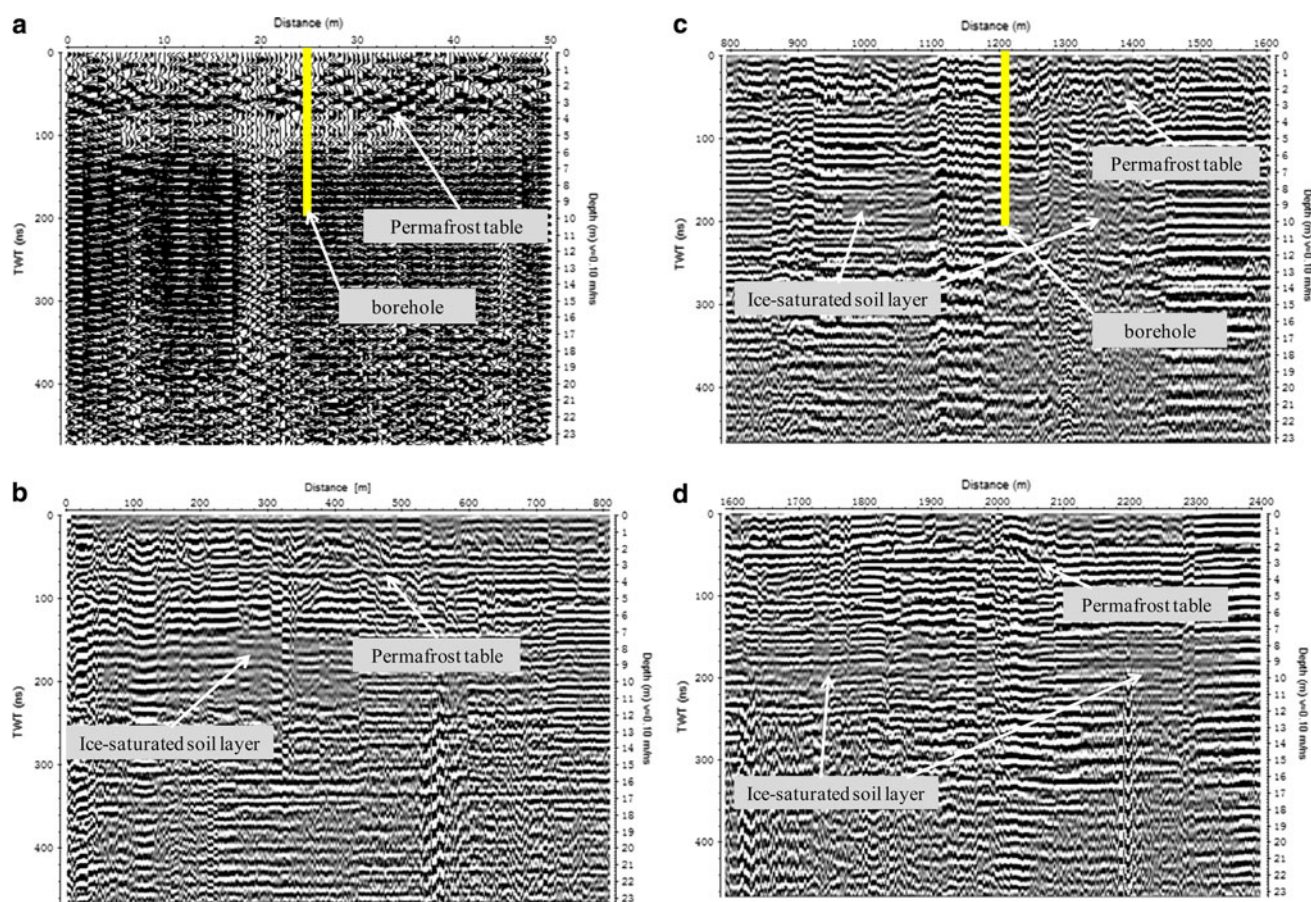


Fig. 9 **a** The interpreted GPR image of the short transect near the drilling borehole using 100 MHz shielded antenna in wiggle mode to show the approximate location of permafrost table. **b** The GPR transect collected using 100 MHz unshielded RTA between the

longitudinal distance of 0–800 m. **c** The GPR transect collected using 100 MHz unshielded RTA between the longitudinal distance of 800–1,600 m. **d** The GPR transect collected using 100 MHz unshielded RTA between the longitudinal distance of 1,600–2,400 m

borehole. The plot options of the interpreted GPR image were set to show the record in wiggle mode, where all the curved waves are visual, as this configuration could enhance the interpretability of the GPR image for a short transect. It is evident that a relatively continuous and strong reflection occurs at the depth between 3.0 and 4.0 m. The bottom of the reflection (4.0 m) was interpreted as the interface of frozen-thawed soil layers, which coincides with the borehole drilling records. The relatively weak reflection at a depth ranging from 4 to 6 m corresponds to an ice-rich soil layer. Beneath the ice-rich soil layer, the reflection becomes strong and homogeneous, probably due to the variations in the composition of soil. The interpreted results agree well with the results of ground temperatures measurement and borehole drilling records. Unfortunately, the transition from ice-rich to ice-saturated soil layer could not be identified in the interpreted GPR image. The reason for this may be that the ice-rich and ice-saturated soil layers were relatively homogeneously composed of clay

and the change of ice contents was gradual which could not result in a sharp contrast in electrical properties of soil layer.

Figure 9b–d shows the interpreted GPR transects with 100 MHz RTA for a 2.4 km long distance. In the radar-gram, the reflection signals above the depth of about 3.0 m are undulant and irregularly shaped, which probably implies a moist clay layer. Beneath the depth of the 3.0 m, the reflection displays a clear and approximately surface-parallel stratification, which could be interpreted as a frozen layer. The contact of the moisture clay layer with the underlying frozen sand and gravel deposits could be identified distinctly in Fig. 9b–d. Figure 9b–d also reveals that the location of thermal interface ranges between 2.0 and 4.0 m along the whole GPR transect and the location of thermal interface moves upwards as the transect extends westwards. The reflection signals become considerably weak below the depth of about 7 m. The low amplitudes of these reflection signals indicate an existence of ice-

saturated soil layer from the depth of 7–12 m. However, the distribution of ice-saturated soil layer is discontinuous in the subsurface stratigraphy. Between the longitudinal distance of 860 and 920 m, and 1,110 and 1,180 m in Fig. 9c, a homogeneous reflection layer appears from the ground surface downwards, where it could be free of the frozen layer due to the thermal disturbance of wadi. This inference could be confirmed by the ground surface landscape (Fig. 3). The thickness of ice-saturated soil layer is estimated to be about 5 m in the east of this transect, and about 2–4 m in the middle and west of this profile (Fig. 9b–d). The ice content in the soil layer below the interpreted permafrost table increases as the depth extends downwards until the depth of about 12 m along the whole transect. The 100 MHz RTA turns out to be an effective tool to detect thermal interface of frozen and thawed soil layers. However, the location of the permafrost base could not be identified in the interpreted GPR images probably due to the strong attenuation of clay to the propagation of electromagnetic wave signal.

Conclusions

The combination of conventional methods and GPR investigation has efficaciously revealed internal structure of permafrost at Honhor basin, Mongolia. At the drilling site, both drilling records and GPR investigation indicate that the interface between frozen and unfrozen sediment has been clearly resolved at the depth of 4.0 m. A 0.5–1.0 m thick permafrost layer containing unfrozen water exists according to the drilling records and ground temperatures observation. The ice content increases from permafrost table downwards. Inferring from the observed ground temperatures profile, the thickness of permafrost is estimated to be 24 m and the thermal regime of permafrost is relatively unstable in this region.

The GPR investigation also detected that the permafrost table is located at the depth of 2.0–4.0 m in the study region. The thickness of the ice-saturated clay layer approaches 2.0–5.0 m in spite of discontinuous distribution in the subsurface stratigraphy. Permafrost at Honhor basin is characterized by high ground temperatures and high ice content, which could be vulnerable to ongoing climatic warming and increasing human activities in this region. The expected permafrost degradation in this region would exert significant impacts on the hydrological cycles and nomadic life of local people. The research results herein are expected to provide an important baseline to assess permafrost dynamics in the future. The long-term continuous measurements of ground temperatures at this site would contribute to understanding the response of permafrost to climatic changes in this suburb region.

Acknowledgments The study conducted in this paper is funded by the project “Establishment of Early Observation Network for the Impacts of Global Warming”, sponsored by the Ministry of Environment, Japan. This research is also supported by the Global Change Research Program of China (2010CB951402), the National Natural Science Foundation of China (Grant numbers: 40901042) and the Hundred Talents Program of the Chinese Academy of Sciences (51Y251571). The authors also would like to thank all the staff from the Institute of Geography, Mongolian Academy of Sciences for their logistic supports to the fieldwork. Finally, the constructive suggestions from two anonymous reviewers and editor-in-chief are especially appreciated.

References

- Arcone SA, Lawson DE, Delaney AJ, Strasser JC, Strasser JD (1998) Ground-penetrating radar reflection profiling of groundwater and bedrock in an area of discontinuous permafrost. *Geophysics* 63:1573–1584
- Arcone SA, Prentice ML, Delaney AJ (2002) Stratigraphic profiling with ground-penetrating radar in permafrost: a review of possible analogs for Mars. *J Geophys Res* 107(E11):5108. doi: [10.1029/2002JE001906](https://doi.org/10.1029/2002JE001906)
- Batima P, Natsagdorj L, Gombluudev P, Erdenetsetseg B (2005) Observed climate change in Mongolia. *AIACC workings papers* 12: 1–26
- Brandt O, Langley L, Kohler J, Hamran S (2007) Detection of buried ice and sediment layers in permafrost using multi-frequency ground penetrating radar: a case examination on Svalbard. *Remote Sens Environ* 111:212–227
- De Pascale GP, Pollard WH, Williams KK (2008) Geophysical mapping of ground ice using a combination of capacitive coupled resistivity and ground-penetrating radar, Northwest Territories, Canada. *J Geophys Res* 113:15. doi: [10.1029/2007JF000585](https://doi.org/10.1029/2007JF000585)
- Doolittle J, Nelson F (2009) Characterising relict cryogenic macrostructures in mid-latitude areas of the USA with three-dimensional ground-penetrating radar. *Permafr Periglac Process* 20: 257–268
- Hinkel KM, Doolittle JA, Bockheim JG, Nelson FE, Paetzold R, Kimble JM, Travis R (2001) Detection of subsurface permafrost features with ground-penetrating radar, Barrow, Alaska. *Permafr Periglac Process* 12:170–190
- IPCC (2007) *Climate change 2007: the physical science basis*. In: Solomon S, Qin D, Manning M, Chen Z, Marquis M and co-authors (eds) *Contribution of working group I to the fourth assessment report of the intergovernmental panel on climate change*. Cambridge University Press, Cambridge and New York, 996 pp
- Ishikawa M, Sharkhuu N, Zhang Y, Kadota T, Ohata T (2005) Ground thermal and moisture conditions at the southern boundary of discontinuous permafrost, Mongolia. *Permafr Periglac Process* 16:209–216
- Jin H, Yu Q, Lv L, Guo D, He R, Yu S, Sun G, Li Y (2007) Degradation of permafrost in the Xing’anling Mountains, Northeastern China. *Permafr Periglac Process* 18:245–258
- Moorman BJ, Robinson SD, Burgess MM (2003) Imaging periglacial conditions with ground-penetrating radar. *Permafr Periglac Process* 14:319–329
- Sandmeier KJ (2010) *Reflex 5.5 manual: sandmeier software*, Zipser Strabe 1, D-76227 Karlsruhe, Germany
- Sharkhuu N (2003) Recent changes in the permafrost of Mongolia. In: Phillips M et al (eds) *Proceedings of the 8th international conference on permafrost*. A. A. Balkema, Brookfield, pp 1029–1034

- Sharkhuu N, Sharkhuu A, Romanovsky VE, Yoshikawa K, Nelson FE, Shiklomanov NI (2008) Thermal state of permafrost in Mongolia. In: Kane DL, Hinkel KM (eds) Proceedings of the 9th international conference on permafrost, Institute of Northern Engineering, University of Alaska, Fairbanks, pp 1633–1638
- Sodnom N, Yanshin AL (1990) Geocryology and geocryological zonation of Mongolia. Digitized 2005 by Parsons M.A. Boulder, CO, National Snow and Ice Data Center/World Data Center for Glaciology, Digital Media
- Stevens CW, Moorman BJ, Solomon SM, Hugenholtz CH (2009) Mapping subsurface conditions within the near-shore zone of an Arctic delta using ground penetrating radar. *Cold Reg Sci Technol* 56:30–38
- Tumurbaatar B, Mijiddorj B (2006) Permafrost and permafrost thaw in Mongolia. In: Goulden CE et al (eds) The geology, biodiversity and ecology of lake Hovsgol (Mongolia). Backhuys publishers, Leiden, pp 41–48
- Wu T, Li S, Cheng G, Nan Z (2005) Using ground-penetrating radar to detect permafrost degradation in the northern limit of permafrost area on the Tibetan Plateau. *Cold Reg Sci Technol* 41:211–219
- Wu T, Wang Q, Watanabe M, Chen J, Battogtokh D (2009) Mapping vertical profile of discontinuous permafrost with ground penetrating radar at Nalaikh depression, Mongolia. *Environ Geol* 56:1577–1583
- Yang M, Wang S, Yao T, Gou X, Lu A, Guo X (2004) Desertification and its relationship with permafrost degradation in Qinghai-Xizang (Tibet) Plateau. *Cold Reg Sci Technol* 39:47–53
- Yoshikawa K, Leuschen C, Ikeda A, Harada K, Gogineni P, Hoekstra P, Hinzman L, Sawada Y, Matsuoka N (2006) Comparison of geophysical investigations for detection of massive ground ice (pingo ice). *J Geophys Res*, 111(E06S19):10. doi:[10.1029/2005JE002573](https://doi.org/10.1029/2005JE002573)
- Zhao L, Wu Q, Marchenko SS, Sharkhuu N (2010) Thermal state of permafrost and active layer in Central Asia during the international polar year. *Permafr Periglac Process* 21:198–207